

## Roles of Colloidal Silicon Dioxide Particles in Chemical Mechanical Polishing of Dielectric Silicon Dioxide

This content has been downloaded from IOPscience. Please scroll down to see the full text.

2005 Jpn. J. Appl. Phys. 44 8383

(<http://iopscience.iop.org/1347-4065/44/12R/8383>)

View [the table of contents for this issue](#), or go to the [journal homepage](#) for more

Download details:

IP Address: 130.237.29.138

This content was downloaded on 09/09/2015 at 04:28

Please note that [terms and conditions apply](#).

## Roles of Colloidal Silicon Dioxide Particles in Chemical Mechanical Polishing of Dielectric Silicon Dioxide

Wonseop CHOI and Rajiv K. SINGH<sup>1</sup>

Samsung Electro-Mechanics Co., Ltd., 314, Maetan3-Dong, Yeongtong-Gu, Suwon, Gyeonggi-Do 443-743, Korea

<sup>1</sup>Department of Materials Science and Engineering and Particle Engineering Research Center, University of Florida, Gainesville, FL 32611, U.S.A.

(Received March 16, 2005; accepted May 22, 2005; published December 8, 2005)

Chemical mechanical polishing (CMP) is carried out using slurry particles in contact with a wafer and a pad. The size and distribution of particles between the wafer and the pad play a crucial role in achieving desired CMP performance. Polishing rates and friction forces were measured as a function of particle size and solids loading, and surface finishes of silica wafers polished with colloidal silica particles were analyzed to validate the polishing mechanism. On the basis of polishing rate, friction force and surface finish, polishing occurring at the pad-particles-wafer interface was analyzed and an interfacial contact model was proposed. Understanding the polishing mechanism using colloidal particles makes it possible to achieve desired CMP performance. [DOI: 10.1143/JJAP.44.8383]

KEYWORDS: chemical mechanical polishing, colloidal silica particles, friction force

### 1. Introduction

Chemical mechanical polishing (CMP) has been developed to achieve global planarization of metal and dielectric films in the microelectronic fabrication industry. The CMP process consists of a resilient pad, a wafer to be polished, and an abrasive slurry.<sup>1)</sup> During the CMP process, a rotating wafer is pressed face down onto a rotating polishing pad while a slurry of abrasive particles and chemical additives flows between the pad and the wafer.<sup>2)</sup> The synergistic interaction of mechanical abrasion and chemical reaction leads to removal of material from the wafer, making the CMP process more complicated.<sup>3)</sup> Understanding the synergistic interaction may result in the improvement of CMP performance in terms of global planarization, low defect density, and appropriate removal rate, which significantly depend on slurry polishing conditions. Therefore, more thoroughly understanding the effect of the polishing slurry on the polishing mechanism is critical to achieving a desired CMP performance.

A commonly used CMP system utilizes abrasive particles that are dispersed in a slurry.<sup>1)</sup> The interfacial interaction of abrasive particles dispersed in a slurry is indispensable for desired CMP performance. The polishing rate, surface finish and surface defects are simultaneously affected by slurry particles.<sup>4,5)</sup> The effects of particle size and solids loading on polishing rate and surface finish have been studied to understand the polishing mechanism and achieve optimized polishing performance. Some have proposed that an increase in both particle size and solids loading leads to an increase in polishing rate,<sup>6,7)</sup> while others have suggested that polishing rate is increased as particle size decreases or it is independent of particle size.<sup>5,8)</sup> Zhou *et al.* proposed that polishing rate increases with increasing solids loading and that a maximum polishing rate is achieved using 80 nm colloidal silica particles.<sup>9)</sup> Their work also suggested that the agglomeration of nanosized particles (*e.g.*, 10 and 20 nm) has a detrimental effect on surface finish and reduces polishing rate. Li *et al.* suggested that an increase in specific surface area of colloidal silica particles leads to an increase in silanol group concentration, resulting in polishing rate.<sup>10)</sup> This indicated that an increase in the polishing rate may be achieved by increasing the contact area of colloidal silica particles. Our previous

studies suggested two removal mechanisms with solids loading for various particle sizes:<sup>11)</sup> one is a contact-area-based removal mechanism, the removal rate of which increased with an increase in the total contact area of particles in contact with the wafer surface. The other is an indentation-based removal mechanism, the removal rate of which increased with an increase in the indentation depth of single particles. As has appeared in previous reports, polishing performance in terms of parameters such as polishing rate and surface finish is significantly related to particle size and solids loading. Even though previous studies have provided insights into polishing mechanisms related to particle size and solids loading, consensus has not been achieved on the effects of particle size and solids loading on polishing performance, no polishing mechanism due to colloidal silica particles has been validated, and no investigation into the interfacial interaction during polishing has been carried out.

This study provides insight into the mechanism of silicon dioxide chemical mechanical polishing carried out with slurries containing nanosized colloidal particles. The effects of particle size and solids loading on polishing rate, surface finish, and friction force are described to delineate a polishing mechanism. An advanced micro-contact polishing model is proposed that includes consideration of the interfacial contact of colloidal particles between the pad and the wafer that varied during polishing.

### 2. Experimental

Levasil abrasive silica slurries obtained from Bayer Company were used for this study. Slurries were diluted to 2, 5, 10, 15, and 30 wt % by adding deionized water. The pH was adjusted to 10.5 using 0.1 M HNO<sub>3</sub> and 0.1 M NaOH. The size and distribution of particles were measured using a Honeywell Microtech UPA 150 particle size analyzer utilizing a light scattering technique. The shape and size of particles were directly analyzed by scanning electron microscopy (SEM). Polishing experiments were conducted to validate a polishing mechanism using a Struers Rotopol 31 tabletop polisher. Process conditions for the polishing tests were as follow: downward pressure (4.5, 7.5, 10.5, and 15 psi), rotation speed of the pad and wafer (110 cm/s), and flow rate of slurry (100 ml/min). The polishing samples 1.5 × 1.5 in.<sup>2</sup> were prepared by clipping 8 inch silicon

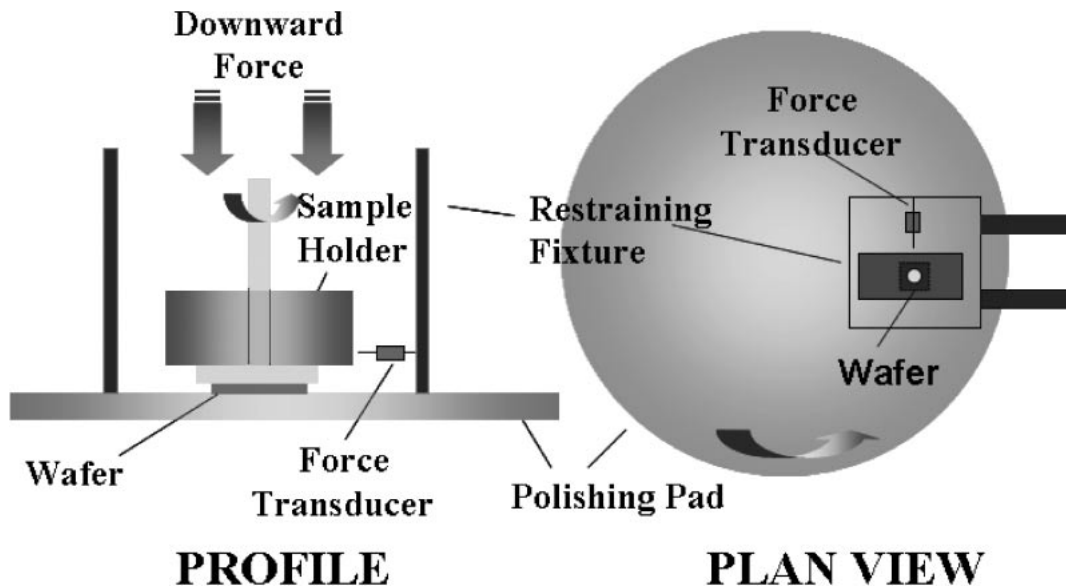


Fig. 1. Schematic presentation of *in situ* lateral friction force instrument.

wafers deposited with silicon dioxide using plasma enhanced chemical vapor deposition (PECVD). The IC 1000/Suba IV stacked pad was utilized as a polishing pad. The polishing pad was conditioned using a Grit-Abrade diamond conditioner to maintain the roughness and porosity of the pad surface. The polishing rate was calculated from the thickness of the silica layer measured using a J. A. Wollan variable angle spectroscopic ellipsometer (WVASE) before and after polishing. The surface topographies and surface roughness of polished layers were characterized using a Digital Instruments Nanoscope III atomic force microscope (AFM).

*In situ* friction force measurements were carried out to delineate the interfacial interaction of particles between the pad and the wafer during CMP. The *in situ* friction force instrument was assembled on the Struers Rotopol 31 tabletop polisher as shown in Fig. 1. Data on the friction force were acquired every 250 ms via a Sensotec model 31 load cell. The friction forces were measured under these conditions: downward pressure (3.5 psi), rotation speed of the pad (110 cm/s), and flow rate of slurry (100 ml/min). The friction forces were measured at intervals of 45 s for each run. De-ionized water was used for a baseline value during the initial 15 s. The variations of friction force due to the addition of slurry containing particles during the next 30 s were normalized against the baseline.

### 3. Characterization

#### 3.1 Size characterization of colloidal silica particles

The size and size distribution of colloidal silica particles is critical in determining polishing performance. As shown in Fig. 2, the particle size distribution measured by light scattering methods showed a well-dispersed colloidal silica with uniform size. Particle size and size distribution were in agreement with the information that the company provided. As shown in Fig. 3, the direct images of colloidal particles detected by scanning electron microscopy (SEM) suggested that colloidal particles were spherical in shape. Particle sizes detected by SEM were in agreement with those measured using light scattering.

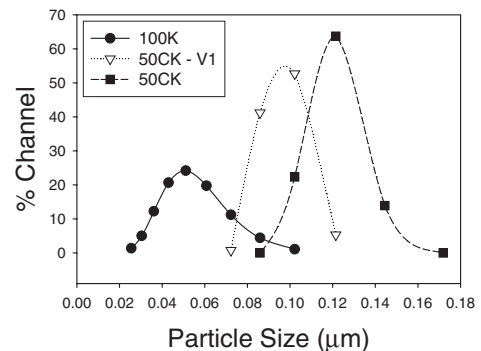


Fig. 2. Particle size distribution for different lots of silica particles diluted in DI water at pH 10.5.

#### 3.2 Surface characterization of polished surface

Surface quality is an indication of the expected yield and reliability of interconnections. A rough interlayer dielectric (ILD) film is more susceptible to low breakdown strength and high leakage.<sup>1)</sup> Roughness is minimized by properly balancing the chemical and mechanical components in the CMP process. The surface characterization of a polished wafer surface needs to be accompanied by polishing tests to obtain an optimized polishing process. The average area and volume of particles in contact with wafer were determined from two parameters containing amplitude and texture information.<sup>12)</sup> Figure 4 shows the surface profile of a cross-sectional area.

As an amplitude parameter that represents the average properties of a profile, surface root mean square (RMS) roughness is given by

$$R_q = \sqrt{\frac{1}{L} \int_0^L Z^2(x) dx}, \quad (1)$$

where  $L$  is the evaluation length and  $Z(x)$  is the height function. Surface RMS roughness is the variation in height from point to point on the surface and indicates an average

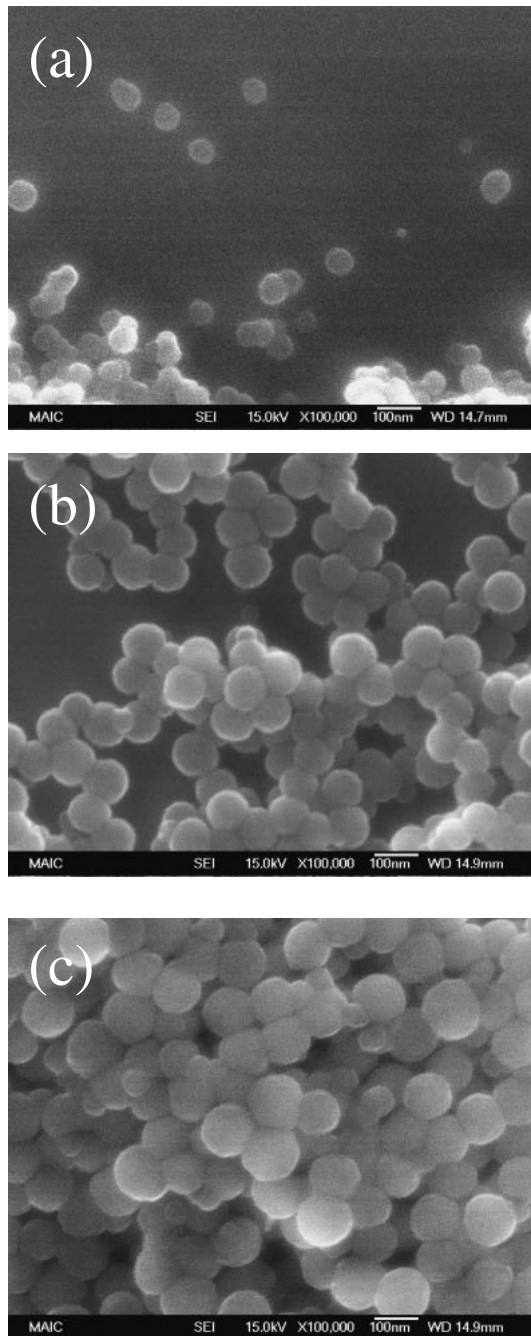


Fig. 3. SEM images of abrasive particles: (a) 100 K, (b) 50 CK-V1, and (c) 50 CK.

indentation depth of particles into the wafer surface. This surface roughness parameter contains no information about the spatial or textural variations in the profile. It is important to describe the variation of relief in the plane of the surface. Texture parameters are utilized to distinguish between the profiles which are visibly different but for which all the amplitude parameters are the same. As a texture parameter, the mean spacing of profile irregularities ( $S_m$ ) is given by the following equation:

$$S_m = \frac{S_{m1} + S_{m2} + S_{m3}}{n}, \quad (2)$$

where  $n$  is the number of peaks per unit length of a profile.  $S_m$  may be a function of particle size and solids loading during polishing.

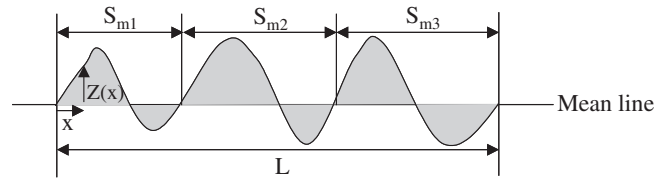


Fig. 4. Surface profile of cross-sectional area of top surface.

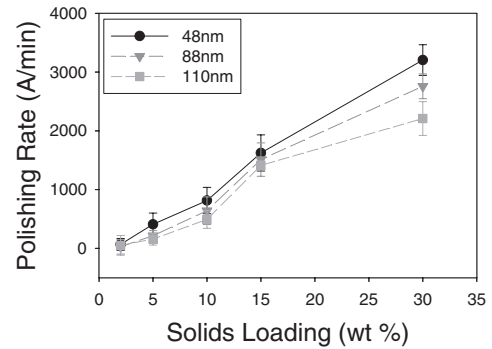


Fig. 5. Polishing rate as a function of solids loading for various particle sizes at condition of downward pressure of 7.5 psi.

#### 4. Results and Discussion

##### 4.1 Polishing rate (solids loading, particle size, and downward pressure effects)

Figure 5 shows polishing rate as a function of solids loading for three kinds of colloidal particles. Polishing tests were conducted at a downward pressure of 7.5 psi. For a given downward pressure, polishing rate may be a function of particle size and solids loading. As seen in Fig. 5, polishing rate increased with a change in solids loading. Because a change in solids loading leads to a variation in the total area of colloidal particles in contact with the wafer surface, an increase in solids loading results in an enhanced polishing rate. For all solids loading conditions, polishing rate may be a function of particle size. A decrease in particle size leads to an increase in polishing rate. For low solids loading ( $\leq 5$  wt %), it is apparent that the difference in polishing rate due to particle size is small. For a high solids loading of 30 wt %, however, polishing rate increased significantly with a decrease in particle size. These differences in polishing rate suggested that the difference in the area of particles in contact with wafer is large under high solids loading conditions. As shown in Fig. 5, a change in polishing rate due to particle size and solids loading is in agreement with a contact-area-based-model.<sup>13)</sup> According to the contact area-based model, polishing rate depends on the total contact area between the abrasive particles and the surface being polished. The contact area as a function of particle size and solids loading is given by the following expression:

$$A \propto C_0^{1/3} \cdot \phi^{-1/3}, \quad (3)$$

where  $A$  is the contact area,  $C_0$  is the solids loading, and  $\phi$  is the particle size. According to this model, the contact area of colloidal silica particles determines polishing rate. Zhou *et al.* reported similar results for polishing by colloidal

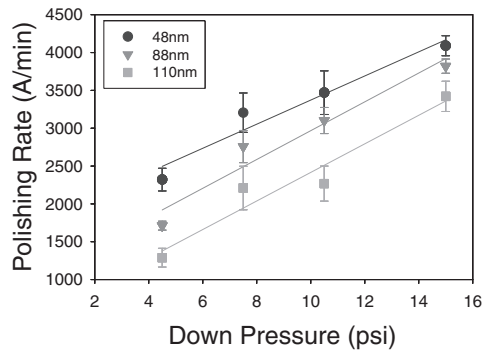


Fig. 6. Polishing rate as a function of downward pressure for various particle sizes.

particles ( $\geq 80$  nm), which showed that polishing rate increases with a decrease in particle size and an increase in solids loading.<sup>9)</sup> For small colloidal particles ( $\leq 50$  nm), they reported that polishing rate decreases with a decrease in particle size because the contact area decreases due to the agglomeration of colloidal particles. Homma *et al.* showed that downward pressure is proportional to downward pressure and polishing rate simultaneously.<sup>14)</sup> This result agrees with the effect of downward pressure on polishing rate for polishing conducted with colloidal silica particles. Consequently, particle size and downward pressure plays an important role in determining polishing rate.

Polishing rate depends significantly on downward pressure, because a change in downward pressure leads to variations in interfacial contact at the pad–particles–wafer interface. Figure 6 shows polishing rate as a function of downward pressure for different particle sizes. Polishing rate was proportional to the down pressure and it increased with a decrease in particle size. Without agglomeration of colloidal particles, the effect of particle size on polishing rate agrees with results from other work.<sup>9)</sup> According to other experiments, agglomeration of colloidal silica particles leads to a lower polishing rate, while this experiment shows no decrease in polishing rate with an increase in particle size because there was no agglomeration confirmed by surface roughness measurements. With increasing downward pressure, polishing rate increased, which follows the model of Preston.<sup>15)</sup> The model of Preston is given by the following equation:

$$\text{MRR} = KPV, \quad (4)$$

where MRR is the material removal rate,  $P$  is the downward pressure,  $V$  is the relative polishing speed, and  $K$  is a system dependent parameter. When the relative velocity and chemical environment remain unchanged, polishing rate is expected to be a function of downward pressure. As seen in Fig. 6, polishing rate follows the model of Preston with some deviation. For the conditions for each particle size,  $K$  is shown on the following Table I.

As shown in Table I,  $K$  is lower at a small particle size than at a large particle size. This explains that the dependence of the CMP system (downward pressure and pad rotation speed) on material removal rate increased with an increase in particle size. It can be concluded that small particles give high removal rates at a designated downward pressure. However, changes in removal rate by downward

Table I.  $K$  (Preston's coefficient) as a function of particle size.

Particle size (nm)	$K$ (1/psi) $\times 10^{-10}$
48	8.3
88	11.2
110	11.3

pressure are lower for small particles than for large particles, a result which is validated by the Preston equation. Consequently, for polishing by colloidal silica particles, optimized polishing rates are tailored on the basis of the dependence of polishing rate on downward pressure.

#### 4.2 Surface characterization (solids loading, particle size, and down pressure effects)

Top-view images and cross-sectional profiles of polished surfaces are an indication of the surface finish produced by chemical mechanical polishing. Surface chemistry, particle size, solids loading, contact area between particles and wafers, and downward pressure simultaneously change the surface finish of the wafer to be polished. Cook proposed a surface roughness model for a single particle located between two hard surfaces in contact.<sup>8)</sup> Surface roughness,  $R_s$ , is the penetration depth of a particle into the surface, which is given by

$$R_s = \frac{3}{4} \cdot \phi \cdot \left( \frac{P}{2kE} \right)^{2/3}, \quad (5)$$

where  $k$  is the particle concentration,  $\phi$  is the particle size,  $P$  is the downward pressure, and  $E$  is the elastic modulus. According to eq. (5), Surface roughness was expected to be a function of particle size, downward pressure, and elastic modulus.

Figure 7 depicts the top-view images and cross sections of silica wafer surfaces polished with colloidal silica particles having diameter of 88 nm for various solids loading: (a) 2, (b) 5, and (c) 15 wt %. The surface roughness (RMS) of the polished surface remained unchanged with an increase in solids loading. The cross section of the polished surface also showed a profile similar to solids loading. The surface roughness (RMS) and the mean spacing of profile irregularities ( $S_m$ ) remained constant with increasing solids loading. When the particle size remains unchanged, surface roughness is a function of downward pressure per particle, as shown in eq. (5). It is clear that downward pressure per particle remains unchanged with an increase in solids loading. Therefore, it can be suggested that the wafer is in contact with the polishing pad and particles embedded into the pad simultaneously. Due to the contact between the pad and the wafer, downward pressure per particle remains unchanged and total contact area does not change at a constant downward pressure.

Figure 8 shows the top-view images and cross sections of silica wafer surfaces polished with colloidal silica particles having diameters of 48 and 110 nm for two solids loading conditions (10 and 30 wt %). For each particle 48 and 88 nm in diameter, surface roughness (RMS) and the mean spacing of profile irregularities ( $S_m$ ) also remained unchanged with solids loading. This shows that downward pressure per particle does not change with solids loading. For each solids

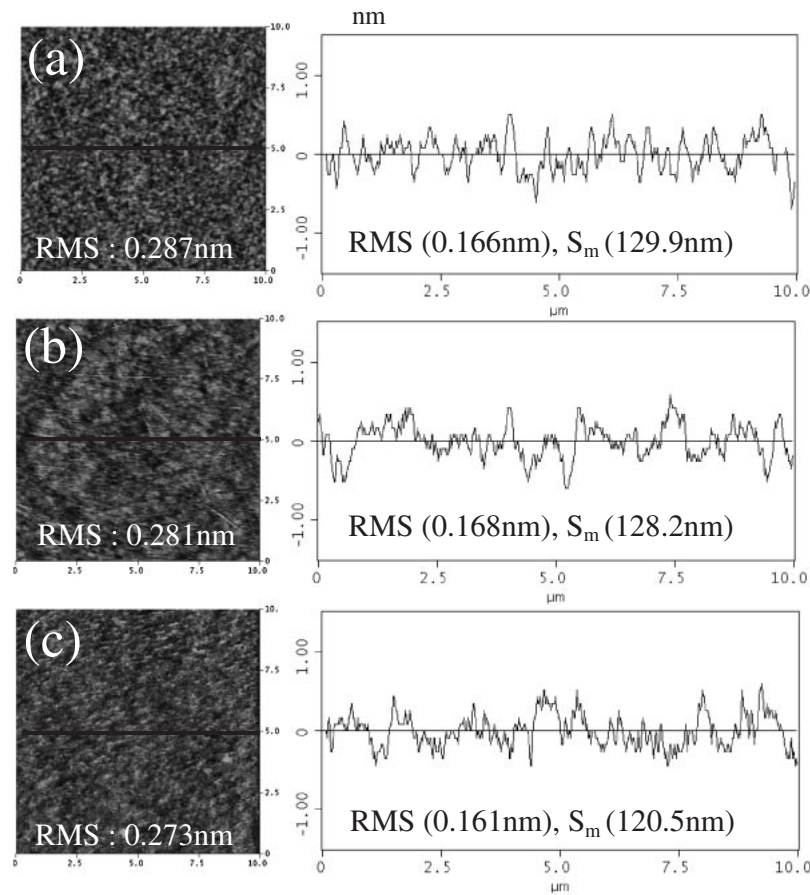


Fig. 7. Top-view images and cross sections of silica wafer surfaces polished with colloidal silica particles having diameter of 88 nm for various solids loading: (a) 2, (b) 5, and (c) 15 wt %.

loading condition, both surface roughness (RMS) and the mean spacing of profile irregularities ( $S_m$ ) increased with particle size. This suggested that an increase in particle size led to an increase in contact area and volume per particle. As shown in eq. (5) and Fig. 8, particle size is a dominant factor in determining surface roughness during CMP.

Downward pressure is expected to be a critical process parameter in determining surface roughness. Figure 9 illustrates the top-view images and cross sections of polished surfaces for various particle sizes and downward pressures. Surface roughness (RMS) and the mean spacing of profile irregularities ( $S_m$ ) remained unchanged with an increase in downward pressure for a given particle size, but they increased with particle size. These results show that downward pressure per particle remains unchanged in spite of the increase in total downward pressure. While the chemical environment (*e.g.*, pH) remained unvaried, the elastic modulus ( $E$ ) of the top surface layer is thought to be constant.<sup>16)</sup> For a constant particle size and chemical environment, surface roughness is a function of downward pressure per particle, as shown in eq. (5). Therefore, this suggests that an increase in downward pressure leads to an increase in contact area between the pad and the wafer, allowing for a constant downward pressure per particle embedded into the pad. Consequently, it is also apparent that particle size is a main contributor to determining surface roughness in the CMP process.

#### 4.3 *In situ* friction force measurements (particle size and solids loading effects)

Friction force is a function of the interfacial contact of particles. Friction force is a measure of how much contact the particles make with the wafer surface, which is important in determining the abrasion mode. For a given solids loading, the change in particle size and solids loading leads to a variation in the interfacial contact of particles in contact with the wafer and the pad. Figure 10 shows friction force as a function of solids loading for various particle sizes. For each solids loading condition, a decrease in particle size allows for an increase in friction force. This suggested that a decrease in particle size leads to an increase in the area of particles in contact with the wafer, resulting in friction force. For each particle size condition, an increase in solids loading enhanced friction force. Friction force raised by an increase in solids loading may be due to an increase in the area of particles in contact with the wafer. In this regard, an increase in the number of particles in contact with the wafer leads to an increase in the area of particles in contact with the wafer, resulting in an increase in friction force and polishing rate.

### 5. Proposed Interfacial Contact Model

An interfacial contact model was proposed to delineate the role of colloidal silica particles at the pad–particles–wafer interface during polishing. One component of the model explains the particle size and solids loading effects on

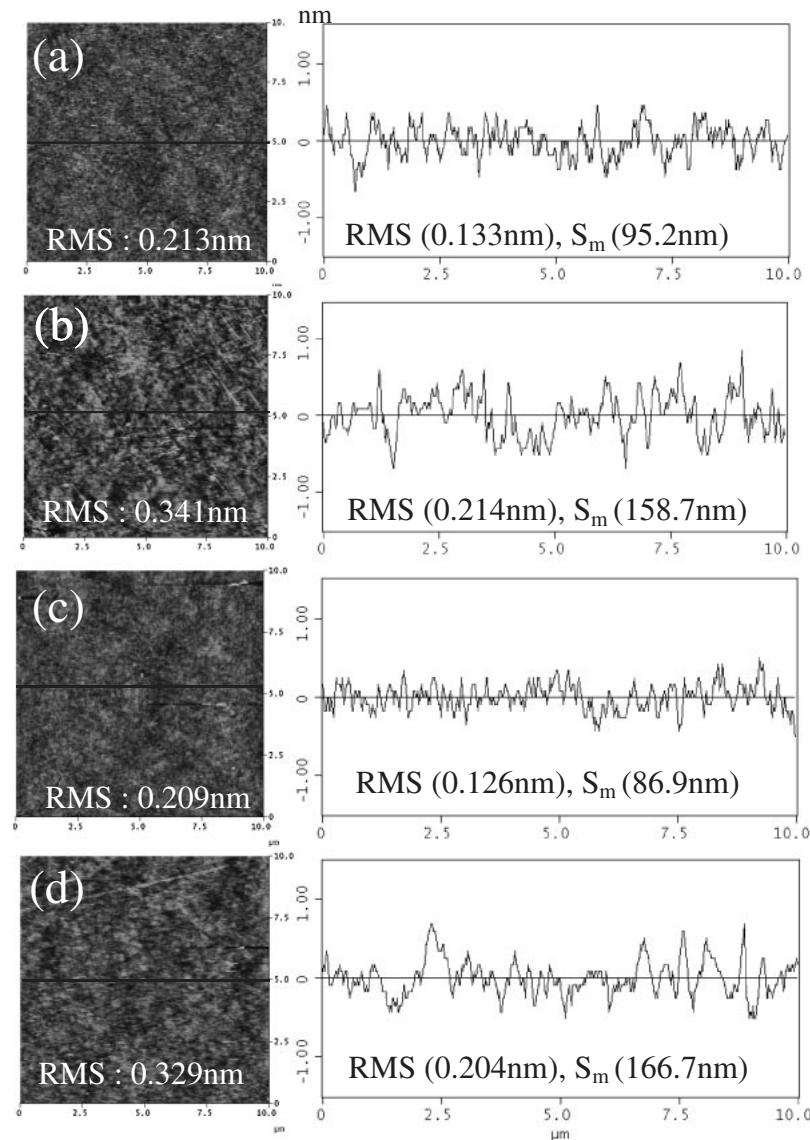


Fig. 8. Top-view images and cross sections of silica wafer surfaces polished with colloidal silica particles for two solids loading conditions: (a) 10 wt % (48 nm), (b) 10 wt % (110 nm), (c) 30 wt % (48 nm), and (d) 30 wt % (110 nm).

interfacial contact that occurs during polishing, and the other component explains the downward pressure effect on the interfacial contact of particles in contact with the wafer and the pad simultaneously.

### 5.1 Particle size and solids loading effects on interfacial contact

Figure 11 shows a schematic diagram of pad–particles–wafer interface as a function of particle size and solids loading. This interfacial contact model was built on the basis of polishing rate, surface finish, and friction force measurements. For given solids loading conditions, the indentation depth of a particle into the wafer surface and contact area per particle increased with particle size, and smaller particles exhibit a higher polishing rate. Even though smaller particles produced shallow indentation depths per particle into the wafer surface, the total contact area of particles in contact with the wafer increased with a decrease in particle size. This suggested that polishing rate increased with the total contact area of particles in contact with the wafer for a

constant solids loading. For a given particle size, indentation depth per particle remained unchanged with an increase in solids loading.

Pressure per particle remained unchanged with increasing solids loading. The wafer was in contact with the pad and the particles embedded into the pad simultaneously during polishing. The polishing rate increased with solids loading for a constant particle size. An increase in solids loading leads to an increase in the number of particles in contact with the wafer, resulting in an enhanced polishing rate.

### 5.2 Downward pressure effects on interfacial contact

Downward pressure is a process input variable in the CMP process. The output parameters such as polishing rate, surface finish, and planarity are determined by modulating the downward pressure. Based on the polishing rate and surface finish of the polished wafer surface, the influence of downward pressure on interfacial contact taking place during polishing is illustrated in Fig. 12. With increasing downward pressure, the asperities of the pad surface go into the pad,

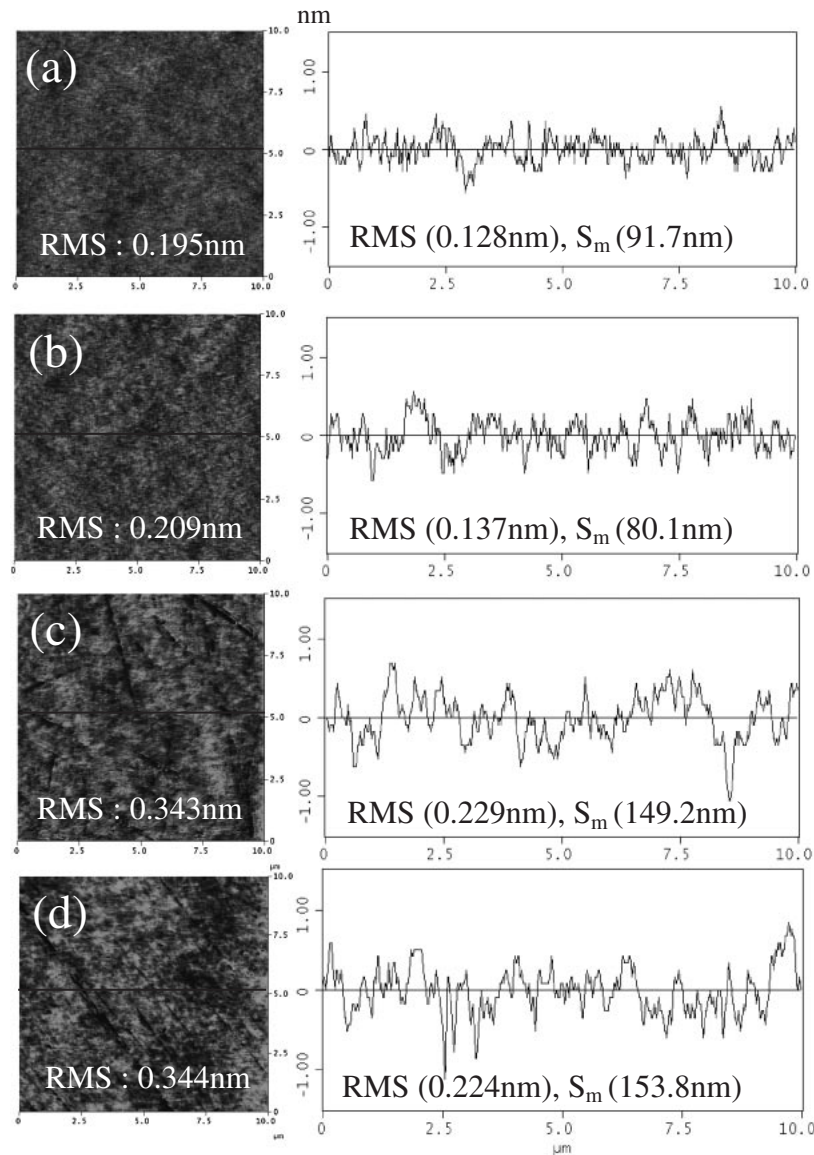


Fig. 9. Top-view images and cross sections of silica wafer surface polished with 30 wt % colloidal silica particles for two different particle sizes and downward pressure conditions: (a) 4.5 psi (48 nm), (b) 15 psi (48 nm), (c) 4.5 psi (110 nm), and (d) 15 psi (110 nm).

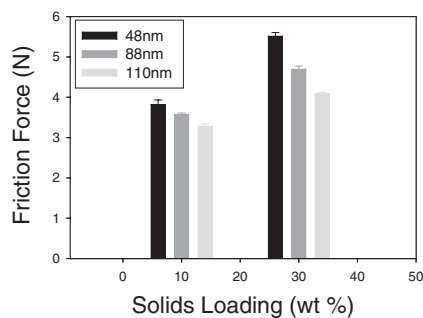


Fig. 10. Friction force as a function of solids loading for various particle sizes.

and the contact area between the pad and the wafer increased, allowing for a large pad–wafer contact area.

The unvaried surface roughness with increasing downward pressure indicated that indentation depth per particle remained unchanged with an increase in downward pressure,

because downward pressure per particle does not markedly increase with increasing downward pressure, which is due to the fact that the wafer comes in contact with the pad and the particles embedded into the pad simultaneously. Consequently, an increase in downward pressure on the wafer can increase the number of particles in contact with the wafer but it does not significantly increase the downward pressure applied to each particle and its indentation depth in the wafer. Therefore, it can be concluded that polishing rate increased with downward pressure due to an increase in the number of particles in contact with the wafer.

### 6. Conclusions

The interfacial interactions of colloidal silica particles between a pad and a wafer were studied to validate a polishing mechanism for dielectric silica. While nanosized colloidal silica particles were inserted into the interface between the pad and the wafer, the polished wafer surface was in contact with the pad and the particles embedded into the pad simultaneously during polishing, which was con-



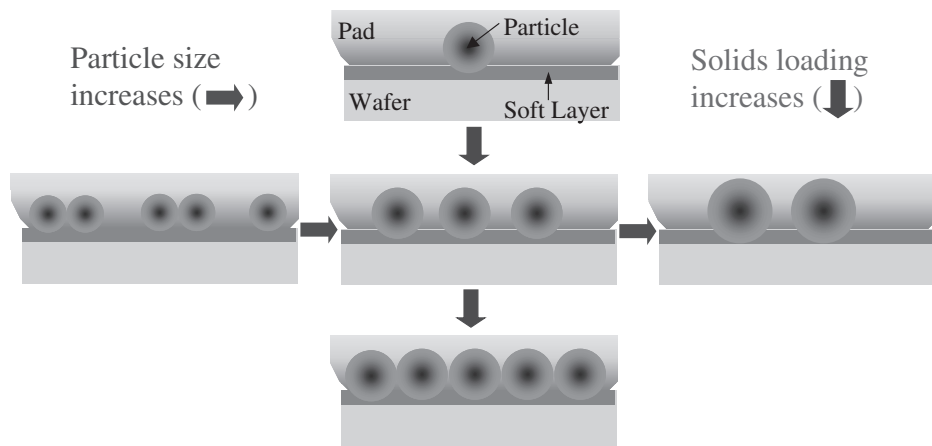


Fig. 11. Schematic diagram of interfacial contact at pad-particles-wafer interface with change in particle size and solids loading.

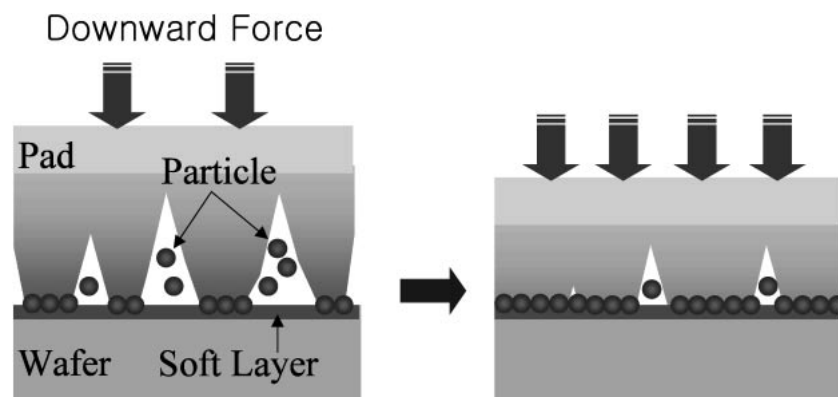


Fig. 12. Schematic diagram of interfacial contact at pad-particles-wafer interface with changes in downward pressure.

firmed by surface finish parameters, such as surface roughness (RMS), and the mean spacing of profile irregularities ( $S_m$ ). In this regard, surface finish did not only remain unchanged with the change in solids loading and downward pressure for a given particle size, but it also increased with an increase in particle size. Polishing rate increased with an increase in solids loading and a decrease in particle size, which indicated that polishing rate increased with an increase in the contact area of colloidal particles between the pad and the wafer.

- 1) J. M. Steigerwald, S. P. Murarka and R. J. Gutmann: *Chemical Mechanical Planarization of Microelectronic Materials* (John Wiley & Sons, New York, 1997).
- 2) R. K. Singh, S.-M. Lee, K.-S. Choi, G. B. Basim, W. Choi, Z. Chen and B. M. Moudgil: *Mater. Res. Bull.* **27** (2002) 752.
- 3) W. C. Oliver and G. M. Pharr: *J. Mater. Res.* **7** (1992) 1564.
- 4) G. B. Basim, J. J. Adler, U. Mahajan, R. K. Singh and B. M. Moudgil: *J. Electrochem. Soc.* **147** (2000) 3523.
- 5) M. Biemann, U. Mahajan and R. K. Singh: *Electrochem. Solid-State Lett.* **2** (1997) 401.
- 6) R. Jairath, J. Farkas, C. K. Huang, M. Stell and S.-M. Tzeng: *Solid State Technol.* **37** (1994) 71.
- 7) R. Jairath, M. Desai, M. Stell, R. Telles and D. Scherber-Brewer: *Mater. Res. Soc. Symp. Proc.* **337** (1994) 121.
- 8) L. M. Cook: *J. Non-Cryst. Solids* **120** (1990) 152.
- 9) C. Zhou, L. Shan, J. R. Hight, S. Danyluk, S. H. Ng and A. J. Paszkowski: *J. Soc. Tri. Lub. Eng. (Apr., 2002)* 35.
- 10) Y. Li and S. V. Babu: *Semiconductor Fabtech* (2003) 13th ed., p. 259.
- 11) U. Mahajan, M. Bielman and R. K. Singh: *Mater. Res. Soc. Proc.* **566** (1999) 27.
- 12) T. Thomas: *Rough Surfaces* (Imperial College Press, 1998).
- 13) M. Biemann: Master's Thesis, University of Florida, 1998.
- 14) Y. Homma, K. Fukushima, S. Kondo and N. Sakuma: *J. Electrochem. Soc.* **150** (2003) G751.
- 15) F. Preston: *J. Soc. Glass Technol.* **11** (1927) 247.
- 16) T. Izumitani: in *Treatise on Materials Science and Technology*, eds. M. Tomozawa and R. Doremus (Academic Press, New York, 1979) p. 115.